Research Article
Experimental and Translational Hepatology

JOURNAL
OF HEPATOLOGY

Targeting the liver clock improves fibrosis by restoring TGF-β signaling

Authors

Emilie Crouchet, Mayssa Dachraoui, Frank Jühling, …, Joachim Lupberger, Atish Mukherji, Thomas F. Baumert

Correspondence

thomas.baumert@unistra.fr (T.F. Baumert), joachim.lupberger@unistra.fr (J. Lupberger).

Graphical abstract

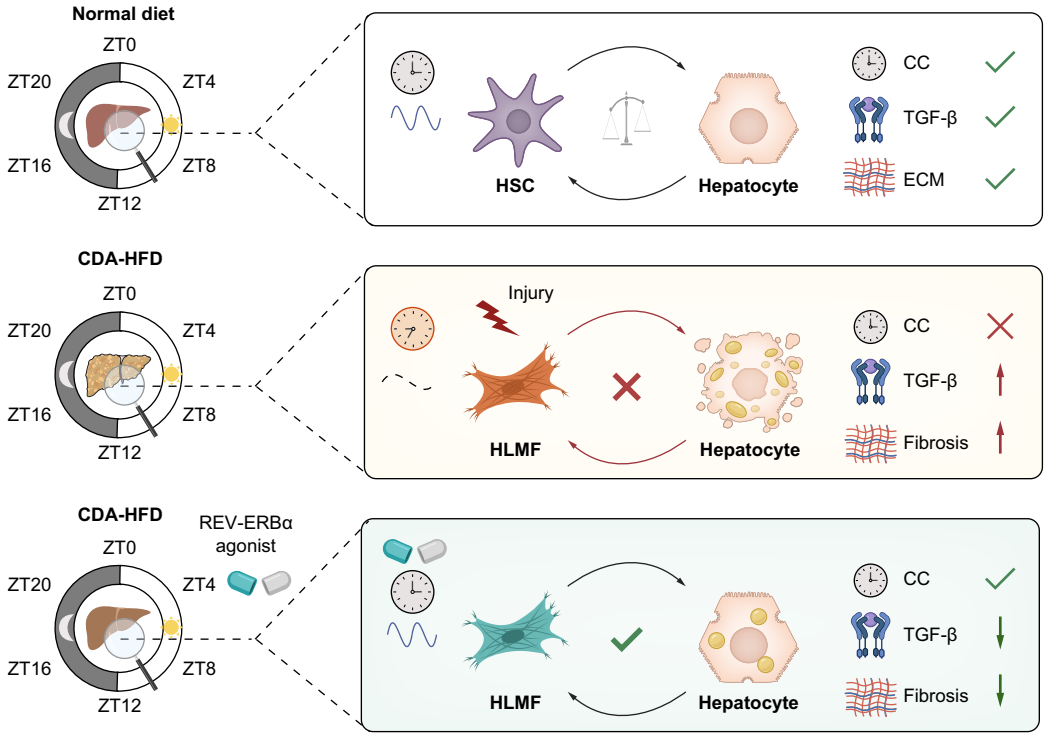

Highlights

- The circadian clock is a regulator of TGF-β signaling in the healthy liver.
- The breakdown of circadian clock control in MASH is associated with liver fibrosis progression.
- Proof-of-concept studies in several models unravel targetability by a small molecule.
- Pharmacological targeting of the circadian clock provides opportunities to improve liver fibrosis.

Impact and implications

Liver fibrosis due to metabolic diseases is a global health challenge. Many liver functions are rhythmic throughout the day, being controlled by the circadian clock (CC). Here we demonstrate that regulation of the CC is perturbed upon chronic liver injury and this perturbation contributes to fibrotic disease. By showing that a compound targeting the CC improves liver fibrosis in patient-derived models, this study provides a novel therapeutic candidate strategy to treat fibrosis in patients. Additional studies will be needed for clinical translation. Since the findings uncover a previously undiscovered profibrotic mechanism and therapeutic target, the study is of interest for scientists investigating liver disease, clinical hepatologists and drug developers.

https://doi.org/10.1016/j.jhep.2024.07.034
© 2024 European Association for the Study of the Liver. Published by Elsevier B.V. All rights are reserved, including those for text and data mining, AI training, and similar technologies. J. Hepatol. 2025, 82, 120–133

Research Article
Experimental and Translational Hepatology

JOURNAL
OF HEPATOLOGY

Targeting the liver clock improves fibrosis by restoring TGF-β signaling

Emilie Crouchet[1,†], **Mayssa Dachraoui**[1,†], Frank Jühling[1], Natascha Roehlen[1,2], Marine A. Oudot[1], Sarah C. Durand[1], Clara Ponsolles[1], Cloé Gadenne[1], Laura Meiss-Heydmann[1], Julien Moehlin[1], Romain Martin[1,3], Nicolas Brignon[1,3], Fabio Del Zompo[1], Yuji Teraoka[4], Hiroshi Aikata[5], Hiromi Abe-Chayama[6,7], Kazuaki Chayama[6,8], Antonio Saviano[1,9], Danijela Heide[10], Mihaela Onea[11], Lucas Geyer[11], Thibaut Wolf[11], Emanuele Felli[1,12], Patrick Pessaux[1,9], Mathias Heikenwälder[10,13,14], Pierre Chambon[15,16], Catherine Schuster[1], Joachim Lupberger[1,*], Atish Mukherji[1,15], Thomas F. Baumert[1,9,17,18,*]

Journal of Hepatology **2025**. vol. 82 | 120–133

Check for updates

Background & Aims: Liver fibrosis is the major driver of hepatocellular carcinoma and liver disease-related death. Approved antifibrotic therapies are absent and compounds in development have limited efficacy. Increased TGF-β signaling drives collagen deposition by hepatic stellate cells (HSCs)/myofibroblasts. Here, we aimed to dissect the role of the circadian clock (CC) in controlling TGF-β signaling and liver fibrosis.

Methods: Using CC-mutant mice, enriched HSCs and myofibroblasts obtained from healthy and fibrotic mice in different CC phases and loss-of-function studies in human hepatocytes and myofibroblasts, we investigated the relationship between CC and TGF-β signaling. We explored hepatocyte-myofibroblast communication through bioinformatic analyses of single-nuclei transcriptomes and performed validation in cell-based models. Using mouse models for MASH (metabolic dysfunction-associated steatohepatitis)-related fibrosis and spheroids from patients with liver disease, we performed proof-of-concept studies to validate pharmacological targetability and clinical translatability.

Results: We discovered that the CC oscillator temporally gates TGF-β signaling and this regulation is broken in fibrosis. We demonstrate that HSCs and myofibroblasts contain a functional CC with rhythmic expression of numerous genes, including fibrogenic genes. Perturbation studies in hepatocytes and myofibroblasts revealed a reciprocal relationship between TGF-β activation and CC perturbation, which was confirmed in patient-derived *ex vivo* and *in vivo* models. Pharmacological modulation of CC-TGF-β signaling inhibited fibrosis in mouse models *in vivo* as well as in patient-derived liver spheroids.

Conclusion: The CC regulates TGF-β signaling, and the breakdown of this control is associated with liver fibrosis in patients. Pharmacological proof-of-concept studies across different models have uncovered the CC as a novel therapeutic target for liver fibrosis – a growing unmet medical need.

© 2024 European Association for the Study of the Liver. Published by Elsevier B.V. All rights are reserved, including those for text and data mining, AI training, and similar technologies.

Introduction

Persistent tissue injury initiates a fibrotic response as a wound healing program. Liver fibrosis is a common step in the pathogenesis of chronic liver disease caused by viral, alcohol-related, and metabolic liver injury. Advanced fibrosis is the major cause of liver disease-related mortality and can lead to hepatocellular carcinoma (HCC), one of the leading causes of cancer-related death.[1] A major obstacle for the development of efficient and safe antifibrotic therapies is the lack of understanding of the mechanisms driving chronic liver disease progression.[2,3]

Due to its high prevalence and rising incidence, metabolic dysfunction-associated steatotic liver disease (MASLD), particularly its progressive form metabolic dysfunction-associated steatohepatitis (MASH), is a major cause of liver fibrosis worldwide. Advanced fibrosis (stage F3, F4) is associated with decompensation, increased HCC risk, and death.[4]

The pathogenesis of liver fibrosis is multi-factorial and mediated by the interplay of hepatocytes, macrophages, and myofibroblasts.[2] While the transforming growth factor-β (TGF-β) pathway has been shown to play an essential role in fibrosis,[2] the molecular mechanisms dysregulating TGF-β-controlled gene expression during fibrosis are only partially understood.

* Corresponding authors. Address: Inserm U1110, 3 Rue Koeberlé, 67000 Strasbourg, France. Tel.: +33 3 68 85 37 03, fax: +33 3 68 85 37 24.
E-mail addresses: thomas.baumert@unistra.fr (T.F. Baumert), joachim.lupberger@unistra.fr (J. Lupberger).
† Authors contributed equally.
https://doi.org/10.1016/j.jhep.2024.07.034

The circadian clock (CC) regulates several functions in the liver. The functioning of the 'clock' largely depends on the CC oscillator, a transcriptional-translational feedback system.[5] The CC oscillator drives daily rhythmicity of its own components as well as that of numerous target genes, through transcriptional, and post-transcriptional mechanisms ensuring liver homeostasis with BMAL1 and REV-ERBα/β as central regulators.[5] While CC perturbation has been shown to be associated with liver disease, the functional role of CC as a driver and therapeutic target for liver fibrosis is unknown.

Materials and methods

Mouse liver HSC isolation

Hepatic stellate cells (HSCs)/myofibroblasts (MFs) were isolated from 8-week-old mice fed with chow diet or choline-deficient, L-amino acid-defined, high-fat diet (CDA-HFD) for 12 weeks. Animals were sacrificed at Zeitgeber time (ZT)0 (7 am), ZT6 (1 pm), ZT12 (7 pm), and ZT18 (1 am). Once the animals were sacrificed, livers were collected and directly processed for MF isolation (see supplementary methods).[18] The experiment (Inserm U1110) was approved by the local ethic committee and authorized by the French ministry of higher education and research (APAFIS#29396-2021012915164103 v2).

Statistical analyses

Individual experiments were reproduced at least 2-3 times, independently (unless otherwise stated). Primary human hepatocytes (PHHs) and human liver myofibroblasts (HLMFs) for *ex vivo* experiments were obtained from tissues of 2-3 independent donors and each condition/treatment was conducted in triplicate. Due to the rarity of patient-fibrotic liver tissues, experiments involving patient-derived fibrotic spheroids were performed one time in triplicate. Each individual values (dots) are presented on the bar charts. GraphPad Prism 8 software was used for statistical analyses. The data are presented as the mean ± SD and were analyzed by the unpaired Student's *t* test or the two-tailed Mann-Whitney *U* test as indicated in figure legends, after determination of distribution by the Shapiro-Wilk normality test. p <0.05 (*), p <0.01 (**), p <0.001 (***) were considered significant. Comparisons of three or more groups were analyzed by ordinary one-way ANOVA followed by Dunnett's or Tukey's multiple comparison tests or Kruskal-Wallis test followed by Dunn's multiple comparison tests as indicated in the legends, after determination of distribution by the Shapiro-Wilk normality test. p <0.05 (* or #), p <0.01 (** or ##), p <0.001 (*** or ###) were considered significant.

Detailed methods are described in the supplementary methods and reagents are listed in the supplementary CTAT table.

Results

The liver CC regulates TGF-β-related gene networks

To investigate the functional role of the liver CC oscillator (Fig. 1A) in the regulation of TGF-β-target gene expression in non-diseased conditions, we first analyzed published circadian transcriptomes from livers of control and *Bmal1* knockout (KO) mice[6] using gene set-enrichment analysis (Fig. 1B).[7,8] In this model, the transcriptional activator *Bmal1* is knocked-out in every tissue including the liver. We found that several TGF-β-target genes and hepatic stellate cell (HSC) activation signatures[9] are rhythmically expressed in control mice (Fig. 1B, Tables S1 and S2), and this regulation is perturbed by *Bmal1* KO (Fig. 1B). We found that profibrotic transcription factors (TFs) *Smad3* and *Atf3* display circadian expression and we observed ultradian transcription patterns for *Col3a1*, *Mmp2*, *Mmp9* and *Mmp13,* which are altered in *Bmal1* KO mouse livers (Fig. S1A). We also performed analyses from livers of hepatocyte-specific *Bmal1* KO mice ($Bmal1^{hep-/-}$) and littermate controls[10] (Fig. 1C). In control livers, both hepatocyte- and HSC-enriched TGF-β-targets are rhythmically expressed (Fig. 1C). Importantly, in $Bmal1^{hep-/-}$ livers, the circadian expression of these TGF-β targets and of the *Bmal1*-controlled CC gene *Rev-Erbα* was abrogated (Fig. 1C). Chromatin immunoprecipitation-quantitative PCR was used to analyze DNA-binding of BMAL1 and its partner CLOCK (Fig. 1A), revealing their rhythmic recruitment to promoter-enhancers of TGF-β targets (Fig. 1D), a pattern identical to its binding to *Dbp* and *Rev-Erbα*. In $Bmal1^{hep-/-}$ livers, BMAL1/CLOCK-binding to these TGF-β targets was lost (Fig. 1D). Analyses of BMAL1/CLOCK-genome-wide binding in mouse livers[9] also confirmed its binding to *Smad7* and *Smad3* (Fig. S1B).

We then evaluated the relationship between the CC and TGF-β targets by analyzing their expression in the liver of hepatocyte-specific *Rev-Erbα/β* KO (Rev-Erbα/β$^{hep-/-}$; LDKO) mice.[11] Transcript analyses showed altered circadian expression of known profibrotic genes (Fig. 1E and S1C). In addition, we found a circadian variation of plasma TGF-β levels, which likely originates from multiple tissues including the liver, correlating with a diurnal activation of SMAD2 and 3 (pSMAD2/3), and increased levels of other TGF-β targets in mouse livers (Fig. S1D,E). ChIP assays revealed that the binding of SMAD2/3/4 to their cognate SMAD binding elements in *Smad7*, *Acta2,* and *Tgfbr1* is circadian and that the parallel recruitment of RNA polymerase II was reduced in $Bmal1^{hep-/-}$ livers (Fig. S2A-C). Additionally, our analyses of an HSC-specific transcriptional signature which includes several TGF-β target genes[12] revealed that their murine orthologues have a rhythmic expression in control livers, and this rhythmicity was disrupted upon *Bmal1* KO (Fig. 1B and Table S2). Finally, we also analyzed the circadian transcription of several genes regulating TGF/BMP/Activin pathways (SMAD-dependent and -independent manner)[13] from whole liver tissue of control and *Bmal1 KO* mice, revealing rhythmic 24-hour expression of key members of these pathways (Figs S3-4). These data suggest that pathways beyond TGF are also at play.

Collectively, these results suggest that the liver CC oscillator controls the duration of expression (circadian gating) of TGF-β target genes in the healthy liver. Hepatocytes are most likely the main contributors to the modulated gene expression. Given the hepatocyte-*Bmal1*-dependent modulation of the circadian expression of HSC-enriched genes (Fig. 1), we also speculate that the hepatocytic CC might indirectly regulate gene expression in non-parenchymal liver cells such as HSCs.

Metabolic stress in PHHs impairs expression of CC genes

The pathogenesis of MASH begins with metabolic alterations, *e.g.*, free fatty acid (FFA) accumulation-induced injury of

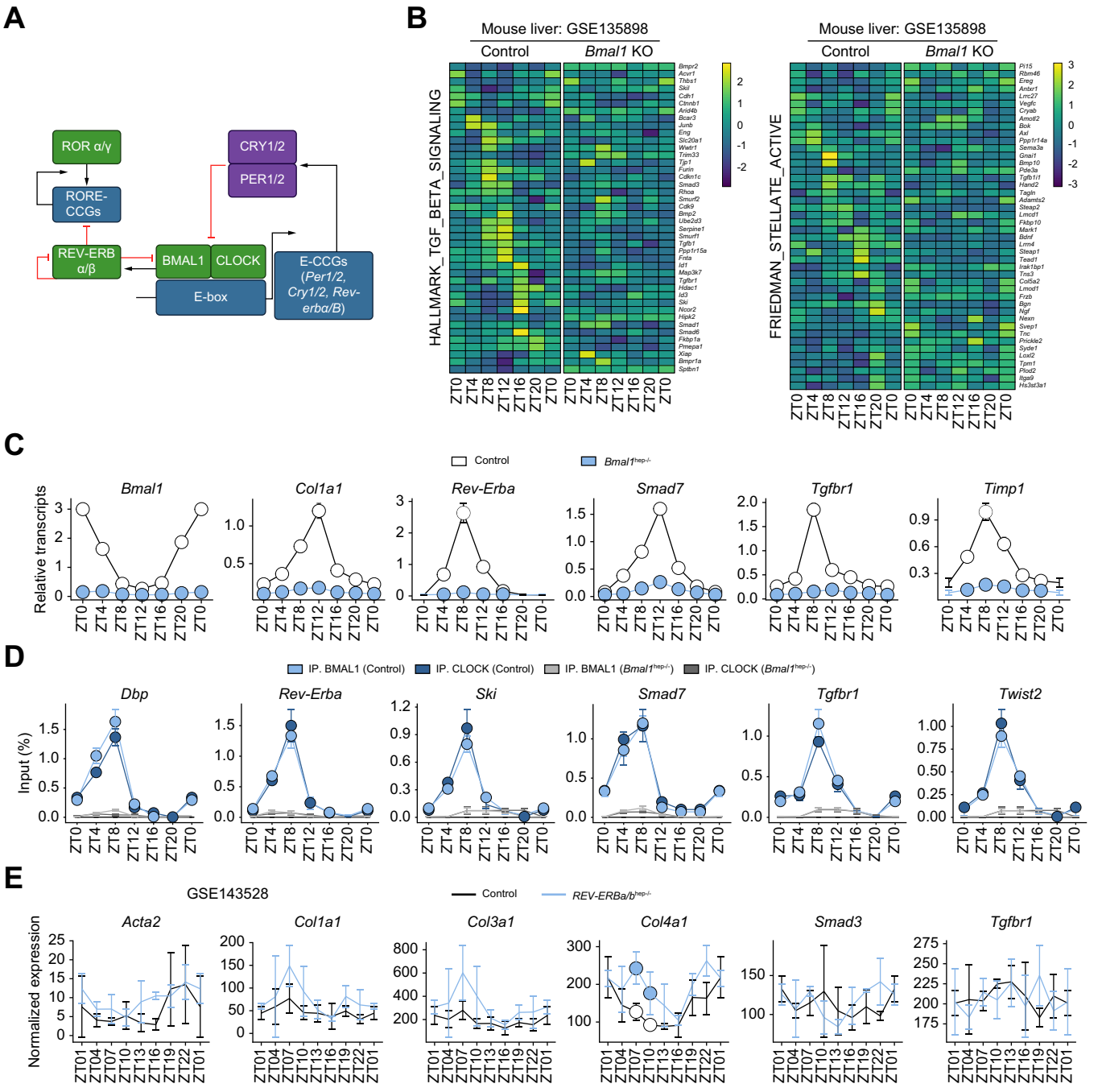

Fig. 1. TGF-β signaling-related genes display circadian rhythmicity in the mouse liver. (A) Model of the CC oscillator. (B) Heatmaps showing expression of HALLMARK TGF-β gene sets (left panel) and murine orthologues of human HSC-specific genes[9] (right panel) in the livers of control and *Bmal1* KO mice (GSE135898).[6] (C) Normalized transcript levels of indicated genes in livers of control and *Bmal1*$^{hep-/-}$ mice.[10] (D) ChIP-qPCR of indicated genes using control and *Bmal1*$^{hep-/-}$ livers[10] and indicated antibodies. (E) Normalized expression of indicated genes in control and *Rev-Erbα/β*$^{hep-/-}$ livers (GSE143528).[11] Data are expressed as mean ± SD. Fig. 1C,D were performed from same control and *Bmal1*$^{hep-/-}$ mice. Three mice/time-point/group. Fig. 1C,D: unpaired Student's *t* test; bold dots: p <0.05. Fig. 1E: Wald test and Benjamini-Hochberg correction; bold dots: FDR <0.05. Refer to Tables S1 and S2. CC, circadian clock; ChIP-qPCR, chromatin immunoprecipitation-quantitative PCR; FDR, false discovery rate; HSCs, hepatic stellate cells.

hepatocytes. To model the status of CC genes in human hepatocytes during MASH, we treated PHHs with FFAs resulting in lipid accumulation (Fig. 2A–C) and perturbation of the expression of several CC components (Fig. 2D and S5A). In synchronized PHHs, FFA treatment altered the rhythmic expression of *BMAL1* and *REV-ERBA* (Fig. 2C). FFAs also increased the expression of TGF-β targets (Fig. 2D–F and S5A). Importantly, pharmacological inhibition of TGF-β activity with SB505124 significantly reduced FFA-induced changes in the expression of CC components and TGF-β targets (Fig. 2G). Next, we explored the relationship between activated REV-ERBs and TGF-β target expression. In FFA-treated PHHs, we

found that treatment with the REV-ERB agonist SR9009[14] prevented (i) lipid accumulation, (ii) alteration of CC gene expression, and (iii) induction of TGF-β targets (Fig. 2H–K). A part of the inhibitory effect of SR9009 persists in a gene-specific manner even with *REV-ERBA* silencing (Fig. S5B,C), possibly reflecting a 'trans-repressive' effect through HDAC3 or other targets.[15,16]

Collectively, our results suggest REV-ERBα as a negative regulator of TGF-β signaling in PHHs and show that metabolic alterations can perturb the expression of CC genes.

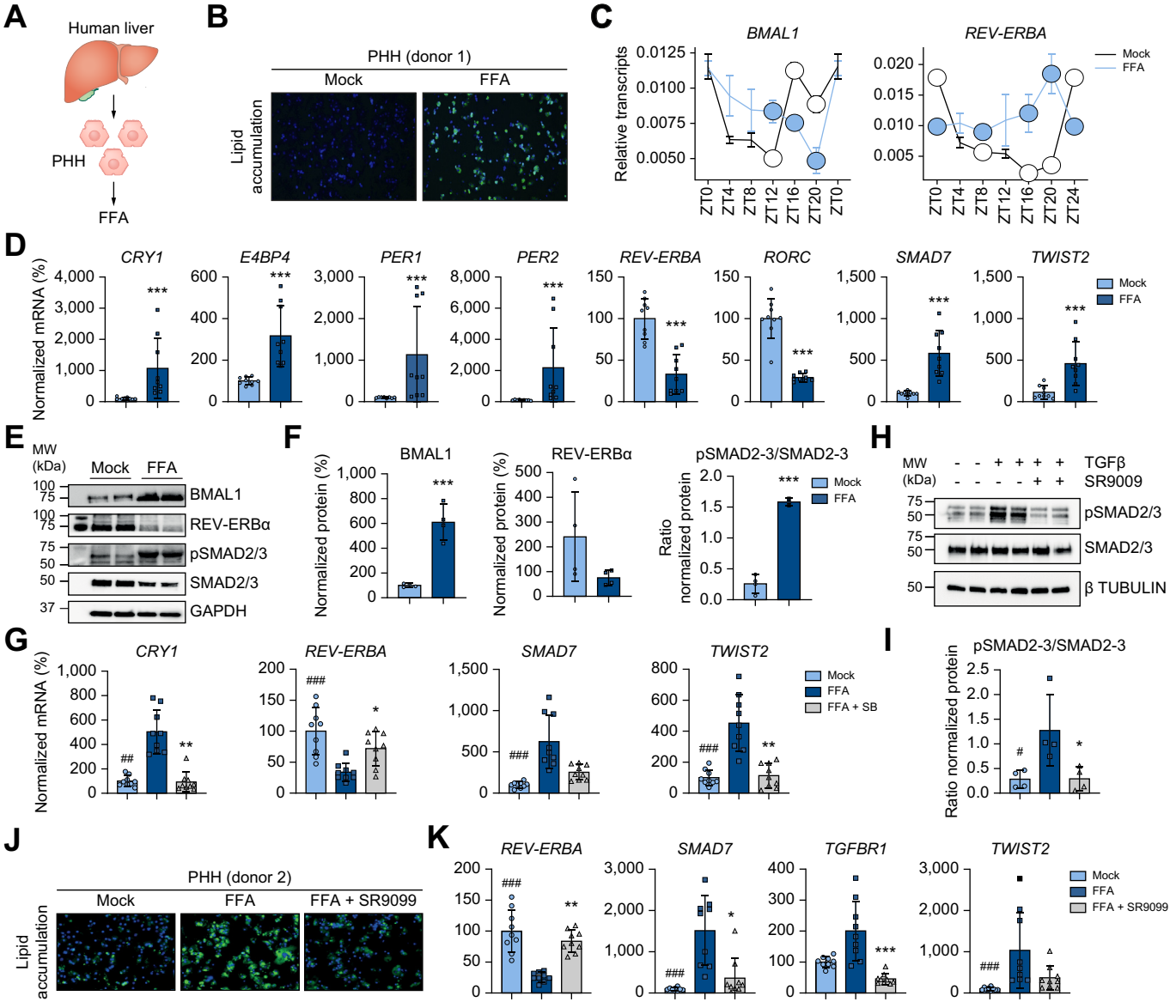

Fig. 2. FFAs drive CC perturbation and induce TGF-β pathway gene expression in PHHs. (A) PHHs were isolated from non-diseased patient livers and treated with FFAs. (B) BODIPY staining confirms lipid accumulation in FFA-treated PHHs. Green = neutral lipids. Blue = DAPI. The pictures show representative image (magnification x10). (C-D) FFA treatment perturbs CC gene expression and rhythmicity in PHHs. (C) The graphs show relative gene expression of *BMAL1* and *REV-ERBA* from synchronized PHHs (low glucose) post-FFA treatment. One representative experiment out of two is shown. Unpaired Student's *t* test; bold dots represent p <0.05. (D) The graphs show means ± SD of % of mRNA normalized to *GAPDH* (mock = 100%) from three experiments performed in triplicate (n = 9). *p <0.05, **p <0.01, ***p <0.001, Mann-Whitney *U* test. (E-F) FFA treatment dysregulated the CC and activates TGF-β signaling in PHHs. One representative experiment in duplicate out of two if shown (see Fig S.17). Quantification of western blot analysis was performed using ImageLab. ***p <0.001 (unpaired Student's *t* test) (G) TGF-β inhibitor reverts FFA-induced dysregulations in PHHs. The graphs show mean ± SD of % of mRNA normalized to *GAPDH* (mock = 100%) from three experiments performed in triplicate (n = 9). *,#p <0.05, **,##p <0.01, ***,###p <0.001 Kruskal-Wallis followed by Dunn's multiple comparison tests (FFA *vs.* mock or FFA-SB *vs*. FFA). (H–K) Perturbation studies in PHHs using the REV-ERBα agonist SR9009. (H–I) One representative experiment in duplicate out of two is shown (see Fig S18). Quantification of western blot analysis was performed using ImageLab. # or *p <0.05 (one-way ANOVA followed by Tukey's multiple comparisons tests). (J) BODIPY staining in PHHs (magnification x10). (K) SR9009 restores FFA-induced dysregulation of CC gene expression. PHHs were treated with FFA and SR9009 or DMSO as control. The graphs show mean ± SD of % of mRNA normalized to *GAPDH* (mock = 100%) from three experiments performed in triplicate (n = 9) *,#p <0.05, **,##p <0.01, ***,###p <0.001 Kruskal-Wallis followed by Dunn's multiple comparison tests (FFA *vs*. mock or FFA SR9009 *vs*. FFA). CC, circadian clock; FFAs, free fatty acids; PHHs, primary human hepatocytes.

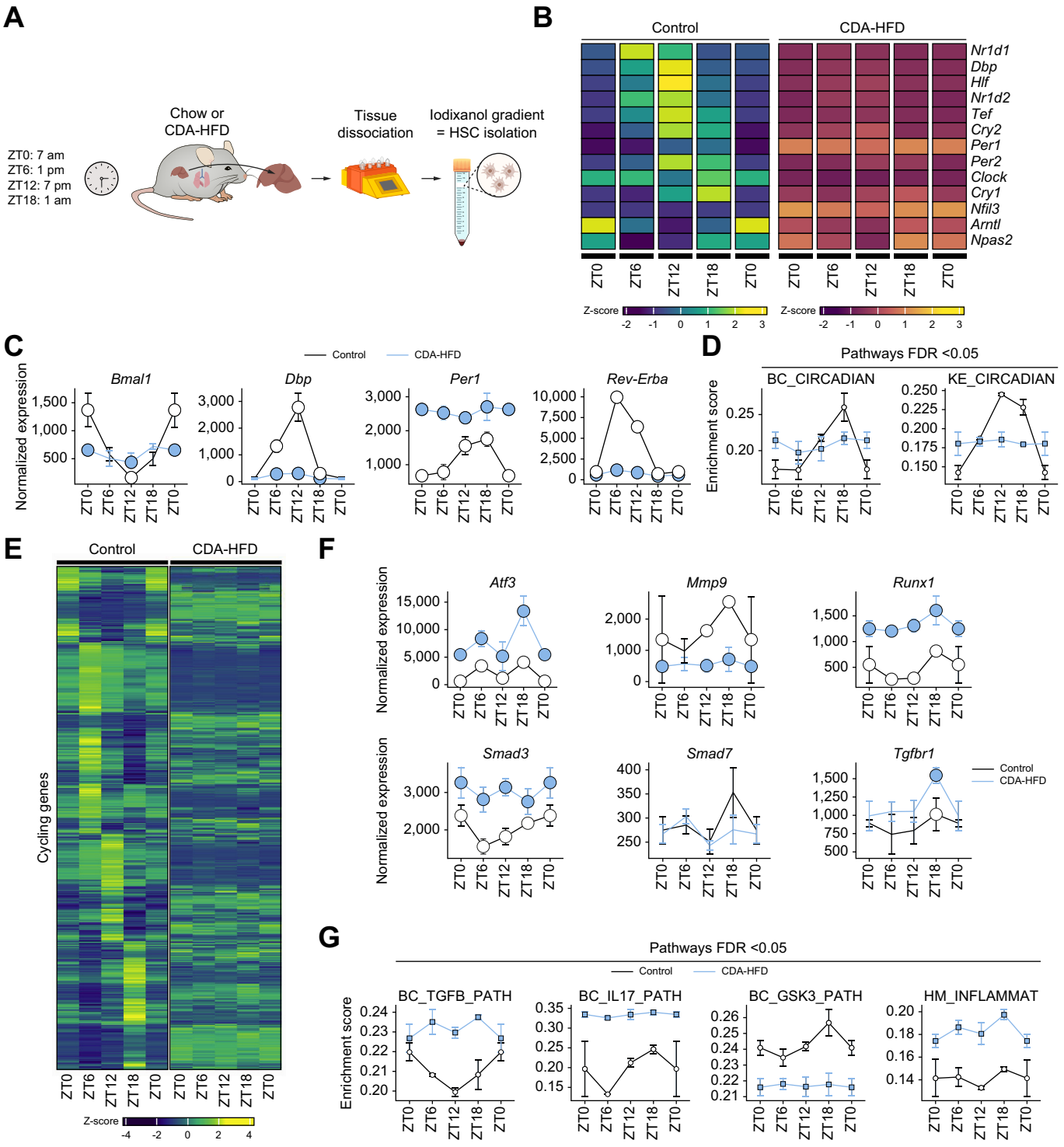

Fig. 3. Diurnal rhythmicity of gene expression is lost in HSCs during fibrosis *in vivo*. (A) Experimental approach showing HSC and MF isolation from mouse livers at different time points from control (chow diet) or CDA-HFD animals (n = 3 animals per group/time-point). (B–G) Diurnal rhythmicity of gene expression is lost in HSCs/MFs during MASH *in vivo*. (B) Heatmap and (C) normalized expression levels of indicated CC genes in control and CDA-HFD HSCs/MFs. (D) Status of circadian pathways (FDR <0.05) in control and CDA-HFD HSCs/MFs. (E) Heatmap of circadian gene expression in control and CDA-HFD HSCs/MFs. (F) Pathways enriched (FDR <0.05) for circadian genes in control HSCs. (G) Circadian enrichments of indicated pathways (FDR <0.05) in control and CDA-HFD HSCs. Panels C, G: Wald test and Benjamini-Hochberg correction; bold dots: FDR <0.05. Refer to Tables S1 to S7. CDA-HFD, choline-deficient, L-amino acid-defined, high-fat diet; CC, circadian clock; FDR, false discovery rate; HSCs, hepatic stellate cells; MFs, myofibroblasts.

Perturbation of circadian rhythmicity in HSCs correlates with fibrotic gene expression *in vivo*

HSCs/MFs are the central effectors of fibrosis.[2,3] While the rhythmic CC oscillator in mouse hepatocytes is well characterized,[5,6,9,11] the existence and status of this CC oscillator in these cells during liver disease remains unknown.

Analysis of a single-nuclei RNA-sequencing (snRNA-seq) dataset from normal mouse liver[11] identified cell-specific markers and CC genes in HSCs (Fig. S6A,B). Employing a CDA-HFD mouse model recapitulating features of MASH-induced fibrosis,[17] we evaluated the status of HSC/MF CC. We isolated and characterized HSCs from mouse livers during circadian rest and active phases[18] (Fig. 3A and S7A,B). Transcriptomic analyses revealed that in HSC, CC genes display characteristic rhythmicity (Fig. 3B,C). The maximum expression of *Bmal1* is observed at ZT0 which when accumulated to sufficient level drives the transcription of its targets like *Dbp, Nr1d1* and *Per1/2* during the rest phase[11] (Fig. 3B,C). In contrast, MFs from fibrotic livers of CDA-HFD mice displayed a perturbed CC oscillator (Fig. 3B,C). Transcriptomic analysis identified 1,994 diurnally expressed genes (~5% of total genes covered) in HSCs, which lost their rhythmicity in CDA-HFD mice (Fig. 3D,E and Tables S3-S4). In control HSCs, the basal level of expression of fibrosis-related genes displayed a diurnal or ultradian rhythmicity (Fig. 3F and S7C). In contrast, we observed an upregulation and/or a perturbed rhythmicity of profibrotic genes (*Smad3*, *Tgfbr1*, *Runx1* and *Atf3*) and downregulation of antifibrotic genes (*Smad7* and *Mmp9*) (Fig. 3F).

Further analyzing the significant cycling genes, we performed gene set variation analysis to identify the pathways regulated by CC in HSCs. HSCs displayed diurnal rhythmicity of metabolic, stress response/cytokine signaling, cellular biochemical processes, collagen, and ECM synthesis/remodeling pathways (Fig. S8 and Tables S5-S6). Analysis of the individual genes leading to the enrichment of these rhythmic pathways identified several key TFs, enzymes, and signaling intermediates (Table S7). Importantly, these enriched pathways were significantly (false discovery rate <0.05) perturbed in MFs of CDA-HFD mice, along with upregulation and altered rhythmicity of pathways driving liver fibrosis, including the TGFβ signaling pathway (Fig. 3G). Activation of the TGFβ signaling pathway is mediated through the canonical SMAD2/3-dependent pathway and non-canonical SMAD2/3-independent pathways such as JNK, MAPK or PI3K/AKT.[19] While *Smad3* and *Smad7* display significant circadian variation over time in HSCs, our gene set variation analysis showed that SMAD-independent pathways were not rhythmic (Table S6), indicating that regulation of fibrotic genes is mediated predominantly by the TGFβ-SMAD pathway. Additional analyses of the circadian transcription of genes regulating TGF/BMP/Activin pathways revealed rhythmic 24-hour expression for multiple key members of these pathways and support that pathways beyond TGF may also be at play (Figs S9-S10).

Collectively, these data indicate that HSCs contain a functional CC oscillator with numerous diurnally expressed genes controlling physiological functions, and that metabolic injury disrupts the HSC CC oscillator, promoting the expression of profibrotic genes.

REV-ERBα activation impairs TGF-β signaling in human HSCs and MFs

The functionality of the human HSC CC oscillator and its impact on expression of TGF-β targets was explored by generating CRISPR-Cas9-guided KO of *BMAL1* and *REV-ERBA* in LX2 stellate cells (Fig. S11A). Circadian synchronization demonstrated perturbed expression of CC genes and TGF-β targets in *REV-ERBA* KO and *BMAL1* KO LX2 cells (Fig. 4A and S12-S13). Moreover, *REV-ERBA* KO increases the expression of profibrotic genes (Fig. 4A). Then, HSCs were isolated from patient-derived liver tissues (Fig. 4B). Of note, isolated HSCs quickly acquire characteristics of HLMFs in cell culture. FFA treatment affected expression of CC components in a gene-specific manner (Fig. 4C) and induces upregulation of TGF-β target expression (Fig. 4D). Inhibition of TGFβ signaling using SB505124 restored CC gene expression (Fig. 4E). Furthermore, the REV-ERBα activator SR9009 reduced the phosphorylation of SMAD2/3 in TGF-β-treated HLMFs (Fig. 4F). As observed for PHHs (Fig. 2), a part of the inhibitory effect of SR9009 persisted in a gene-specific manner with REV-ERBA silencing (Fig. S11B).

Collectively, these results indicate a reciprocal relationship between REV-ERBα function and expression of TGF-β targets in HLMFs. This also suggests that activating REV-ERB could dampen TGF-β signaling in liver disease and might attenuate fibrosis progression.

Crosstalk and communication of the hepatocyte CC with HSCs

Since our transcriptomic analyses highlighted a perturbed expression of HSC-enriched genes in hepatocyte-specific CC KO mice (Fig. 1), we aimed to study the impact of CC perturbation in hepatocytes on HSC gene expression. Analysis of snRNA-seq data of livers from LDKO mice[11] revealed ~300 perturbed HSC genes including CC genes (*Bmal1*, *Npas2*, *Rora*, and *E4bp4*), TFs (*Mlxipl*, *Srebf1*, *Pparβ*), metabolic regulators (*Fasn*, *Insig2*, *Acly*), and ligands/receptors (*Nrg4*, *Pi3kr1*, *Pdgfrβ*, *Il1r*) (Fig. 5A,B and Table S8).

To functionally validate a crosstalk between human hepatocyte CC and HLMF-enriched profibrotic gene expression, we knocked-down *BMAL1* (si*BMAL1*) in PHHs and subsequently co-cultured them with HLMFs, treated with TGF-β (Fig. 5C). Specific silencing of hepatocyte *BMAL1* (Fig. 5D) led to a significantly increased expression of HLMF-enriched genes *ACTA2*, *COL27A1* and *TGFB* (Fig. 5E). The magnitude of these changes was donor dependent. Collectively, these results suggest that the hepatocyte CC can influence HSC gene expression, possibly by regulating the levels and activities of different TFs, secretory proteins and receptor-ligand pairs.

Pharmacological targeting of REV-ERBs inhibits liver fibrosis progression *in vivo*

To explore the CC as a therapeutic target for MASH-induced fibrosis, we studied whether SR9009, a pharmacological activator of REV-ERBα,[14] modulates fibrosis in CDA-HFD fed C57Bl/6J mice, a state-of-the-art model for MASH fibrosis (Fig. 6A). We confirmed REV-ERBs target engagement in whole liver tissues by an SR9009-induced decrease of REV-ERBs transcriptional targets *Bmal1* and *Clock* (Fig. 6B). SR9009 treatment resulted in significant inhibition of liver fibrosis as shown by a decrease of collagen deposition (collagen proportionate area) (Fig. 6C,D), hydroxyproline levels (Fig. 6D) and fibrotic gene expression and content (Fig. 6E,G). Liver steatosis and inflammation remained unchanged (Fig. 6F and S14) in line

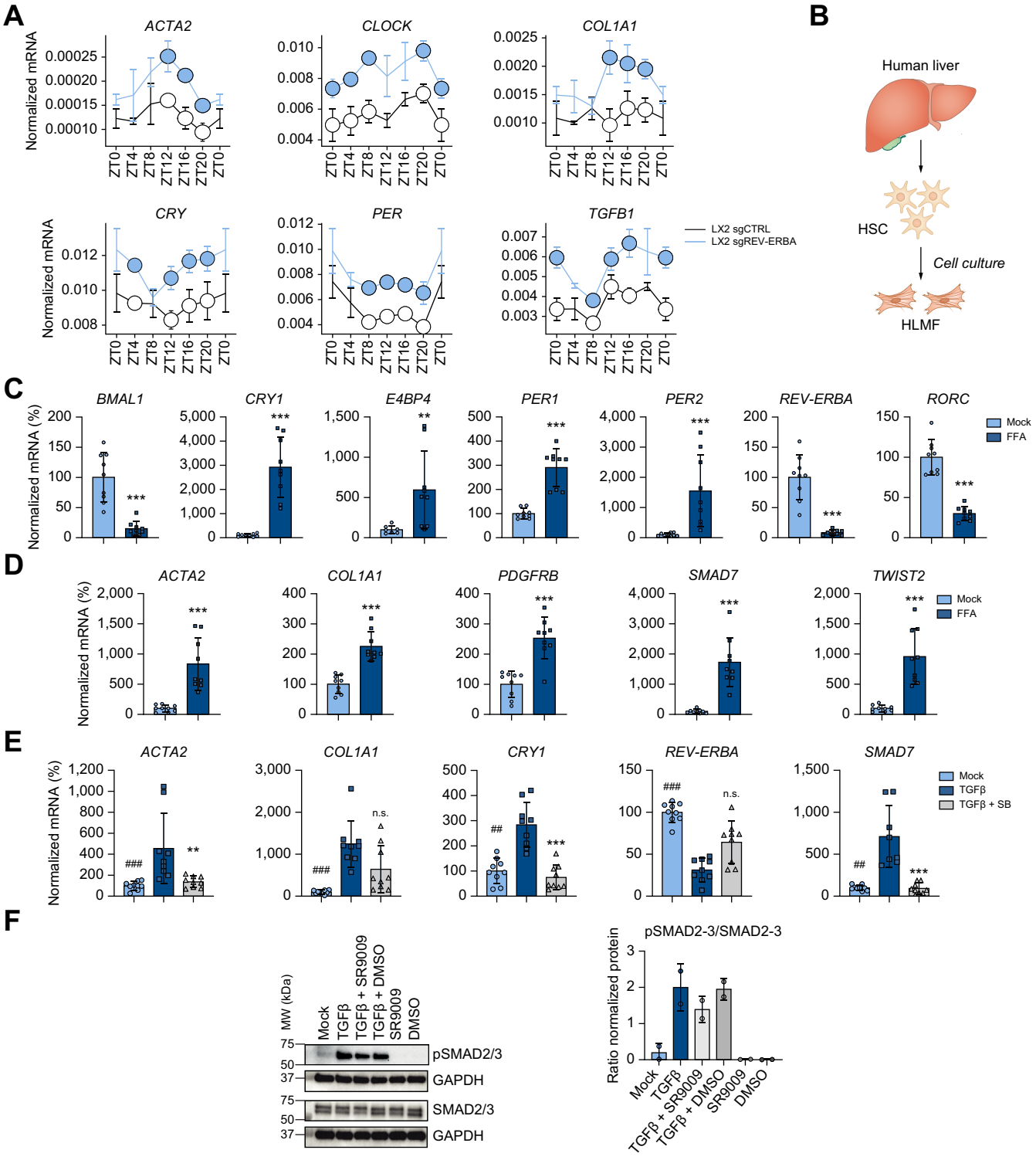

Fig. 4. SR9009 inhibits fibrotic gene expression in HLMFs. (A) Perturbation of CC in LX2 stellate cells induces an increase in fibrotic gene expression. *REV-ERBA* KO LX2 stellate cells were generated and synchronized. The graphs show mean ± SD of relative mRNA expression normalized to *GAPDH* mRNA. One representative experiment out of three performed in triplicate is shown (see Fig. S12-13). Unpaired Student's t-test. Bold dots represent p <0.05. (B) HLMFs were isolated from patient liver tissues and exposed to FFAs. (C-D) FFA treatment perturbs CC gene expression in HLMFs and induces fibrotic gene expression. The graphs show means ± SD of % of mRNA normalized to *GAPDH* (mock = 100%) from three experiments performed in triplicate (n = 9). *p <0.05, **p <0.01, ***p <0.001, Mann-Whitney *U* test. (E) Perturbation of CC and fibrotic gene expression are reversed by the TGFβ inhibitor SB505124. The graphs show mean ± SD of % of mRNA normalized to *GAPDH* (mock = 100%) from three experiments performed in triplicate (n = 9). *,#p <0.05, **,##p <0.01,***,###p <0.001 Kruskal-Wallis followed by Dunn's multiple comparison tests (TGFβ *vs.* mock or TGFβ+SB *vs.* TGFβ). (F) SR9009 inhibits TGF-β signaling in HLMFs. One representative experiment out of two is shown (see Fig S19). Quantification of western blot analysis was performed using ImageLab. CC, circadian clock; KO, knockout; HLMFs, human liver myofibroblasts.

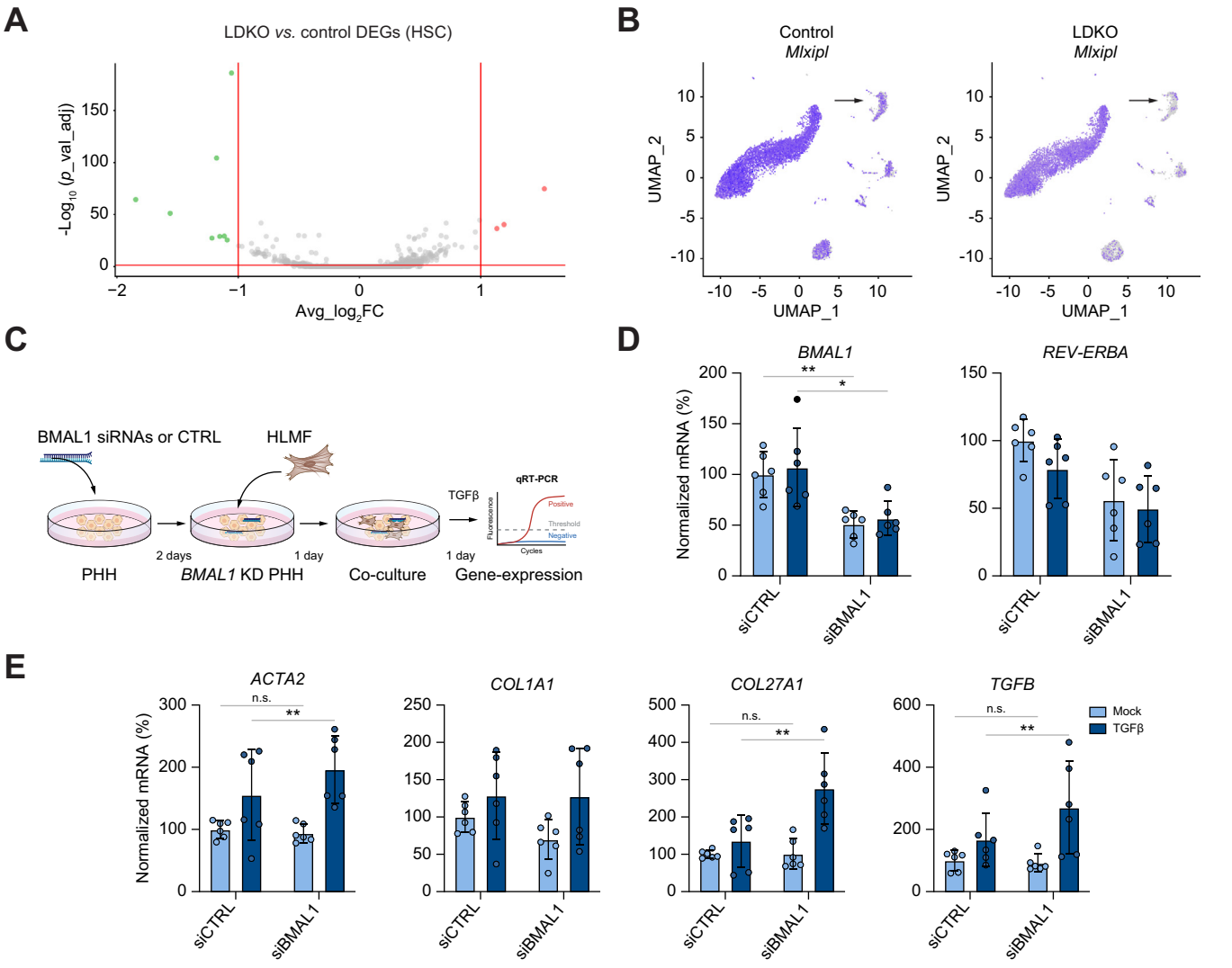

Fig. 5. Crosstalk and communication of the hepatocyte CC with HLMFs. (A) Volcano plot showing differential expression of genes in HSCs of control and LDKO[11] mice. Adjusted p value: Wilcoxon Rank Sum test with Bonferroni correction. (B) Uniform manifold approximation and projection showing expression of *Mlxipl* in different liver cell types in control and LDKO mice. Black arrow = *Mlxipl* expression in HSCs. (C-E) PHH-HLMF co-culture model showing that the perturbation of the hepatocyte CC modulates the HLMF phenotype. (C) Experimental approach (see method). (D-E) The graphs show means ± SD of % of mRNA normalized to *GAPDH* (mock = 100%) from two experiments performed in triplicate (n = 6). **p* <0.05, ***p* <0.01, Mann-Whitney *U* test. Refer to Tables S8. CC, circadian clock; KO, knockout; HLMFs, human liver myofibroblasts; HSCs, hepatic stellate cells; LDKO, hepatocyte-specific KO of Rev-Erbα/β; PHHs, primary human hepatocytes.

with transcriptomic analyses revealing that SR9009 treatment only had a modest effect on lipid metabolism (Fig. S15, Table S9). In contrast, CDA-HFD-driven perturbations of xenobiotic, steroid, and amino acid metabolism were partially restored (Fig. S15, Table S9). Consistent with histopathological analyses, RNA-Seq and CIBERSORTx cell fraction modeling[20] showed similar abundance of the major liver cell populations in treatment and vehicle-treated animals (Fig. S14). Moreover, RNA-Seq/CIBERSORTx analyses revealed reduced levels of *Rev-Erbα* (*Nr1d1*) in hepatocytes of mice subjected to CDA-HFD diet (Fig. 6H–I, Table S9-S10). Upon SR9009 treatment *Rev-Erbα* expression was restored, resulting in decreased expression of its downstream targets *Bmal1, Clock,* and *Cry1* (Fig. 6I).

To validate the therapeutic effect of SR9009 in a mouse model closer to the patient, we applied a human liver chimeric mouse model (HLCM) (Fig. 7A). HLCM are generated using *Fah*$^{-/-}$/*Rag2*$^{-/-}$/*Il2rg*$^{-/-}$ (FRG)-NOD mice with livers repopulated by PHHs expressing human REV-ERBα in the chimeric livers.[21] Feeding HLCM with CDA-HFD recapitulates key features of liver fibrosis. While these mice lack T and B cells, the mouse livers contain macrophages, myofibroblasts and endothelial cells.[21] Immunohistochemistry confirmed the degree of humanization (FAH, Fig. 7B), a lack of T cells (CD3; Fig. S16A), and the presence of macrophages (CD68; Fig. S16A). Treatment of CDA-HFD HLCM mice with SR9009 inhibited liver fibrosis as shown by a decrease of collagen deposition (Sirius red), HSC activation (αSMA), and reduction of fibrotic gene expression (Fig. 7B–E). Lipid accumulation (Oil Red O staining) remained unchanged after SR9009 treatment, as did blood levels of triglycerides and FFAs (Fig. S16B-E). SR9009 treatment had no detectable effect on apoptosis (Fig. S16F-G).

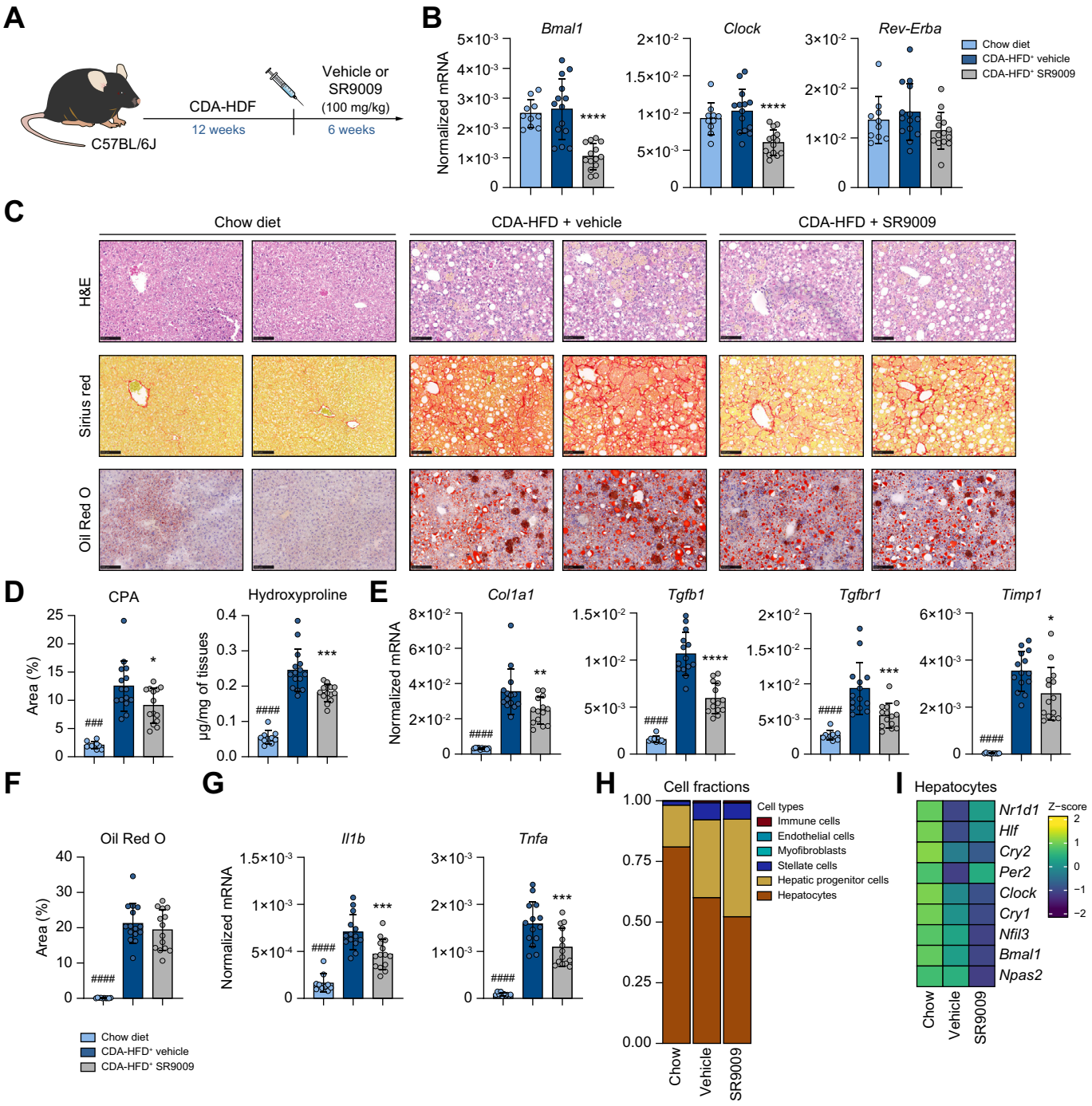

Fig. 6. REV-ERBs agonist SR9009 inhibits liver fibrosis progression in a MASH fibrosis model *in vivo*. (A) Study design. Male C57Bl/6 mice fed with a standard chow diet or CDA-HFD for 12 weeks. Animals received vehicle control or SR9009 for 6 weeks. Chow diet n = 10; CDA-HFD + vehicle n = 15; CDA-HFD + SR9009 n = 14. (B) Target engagement assay. SR9009 treatment efficacy was confirmed by the decrease in *Bmal1* and *Clock* expression, the downstream target of *Rev-Erba*. (C-E) SR9009 treatment improves liver fibrosis. (C) Representative stainings for H&E, Sirius red and Oil Red O are shown (scale bar = 100 µm). Fibrosis levels were evaluated by (D) quantitative digital analysis (CPA), hydroxyproline quantification and (E) fibrotic gene expression measurement. (F) Lipid accumulation by Oil Red O staining quantification. (G) SR9009 treatment reduced expression of *Il1* and *Tnfa* in mouse liver. The graphs show mean ±SD of % area, µg/mg of tissues or relative mRNA expression normalized to *GAPDH* mRNA. $^{*,\#}p$ <0.05, $^{**,\#\#}p$ <0.01,$^{***,\#\#\#}p$ <0.001, $^{****,\#\#\#\#}p$ <0.0001 (vehicle vs. chow or SR9009 vs. vehicle) Mann-Whitney *U* test. (H–I) CIBERSORTx -pathway analyses on mouse liver RNA-Seq were used to predict (H) overall liver cell type abundances and (I) hepatocyte CC gene expression in the indicated study groups. Refer to Tables S9 and S10. CC, circadian clock; CDA-HFD, choline-deficient, L-amino acid-defined, high-fat diet; CPA, collagen proportionate area; MASH, metabolic dysfunction-associated steatohepatitis.

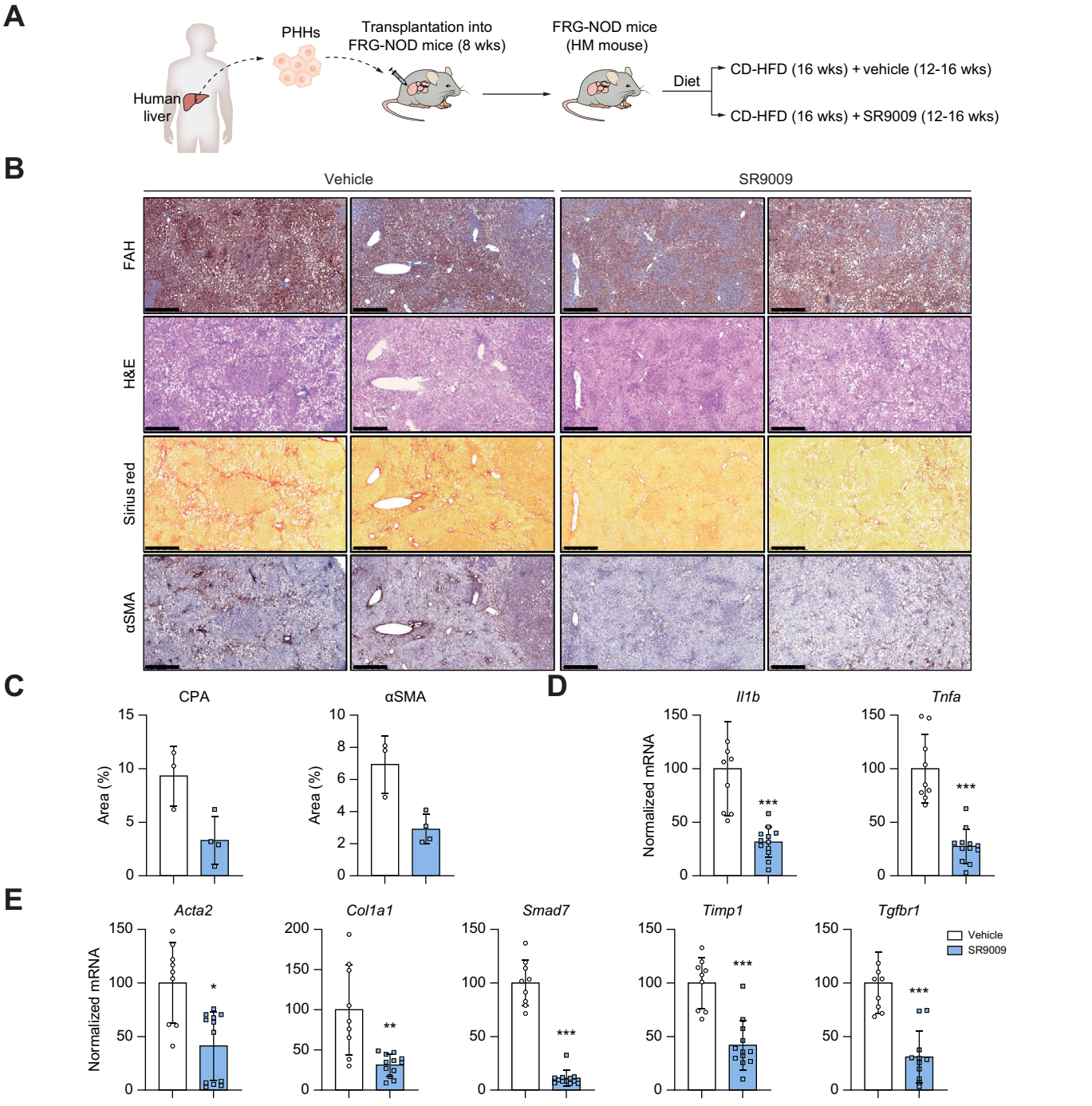

Fig. 7. SR9009 inhibits fibrosis in HLCM. (A) Study design. FRG-NOD mice were engrafted with PHHs to generate HLCM (see method) and subjected to CDA-HFD for 12 weeks. Animals received vehicle control or SR9009 for 4 weeks. CDA-HFD + Vehicle n = 3; CDA-HFD + SR9009 n = 4. (B-D) SR9009 treatment improves liver fibrosis in HLCM. (B) Representative staining images for H&E, Sirius red, FAH and αSMA are shown (scale bar = 500 μm). Fibrosis levels were evaluated by (C) quantitative digital analysis (CPA) and aSMA quantification (% of area) and (D) fibrotic gene expression measurement. (E) SR9009 treatment reduces liver inflammation. The graphs show mean ± SD of % area or relative mRNA expression normalized to *GAPDH* mRNA. *p <0.05, **p <0.01, ***p <0.001, Mann-Whitney U test. CDA-HFD, choline-deficient, L-amino acid-defined, high-fat diet; CPA, collagen proportionate area; HLCM, human liver chimeric mice; PHHs, primary human hepatocytes.

Deregulated expression of CC genes is associated with liver fibrosis progression in patients and SR9009 treatment reduces fibrosis gene expression in patient liver spheroids

Transcript analyses of CC components in patients with metabolic liver disease (GSE126848)[22] showed decreased *PER1*, *PER2*, *REV-ERBs*, and *CRY2* expression, while *CLOCK* expression was increased (Fig. 8A). In a second cohort of patients with MASLD and varying degrees of fibrosis (F0 to F4; GSE135251),[23] we also observed that the expression of *PER1*, *PER2* and *REV-ERBs* was reduced in the liver (Fig. 8B). Reduced *PER1*, *PER2,* and *REV-ERBA* expression was observed in early (F2) and more pronounced in the advanced

stages (F3–F4), most likely due to increase severity of inflammation and fibrosis[23] (Fig. 8B).

Finally, we targeted the CC in patient-derived liver spheroids which include epithelial cells, fibroblasts, and immune cells modeling key features of the liver microenvironment.[24] TGF-β and SR9009 treatment of non-diseased liver tissue-derived spheroids revealed a SR9009-induced rescue of TGF-β-reduced *REV-ERBA* expression (Fig. 8C), and an inhibition of TGF-β target gene expression by SR9009 (Fig. 8C). Remarkably, in fibrotic patient-derived spheroids, SR9009 effectively reduced TGF-β-regulated fibrotic gene expression (Fig. 8D). These results support a clinical impact of CC as a therapeutic candidate for liver fibrosis.

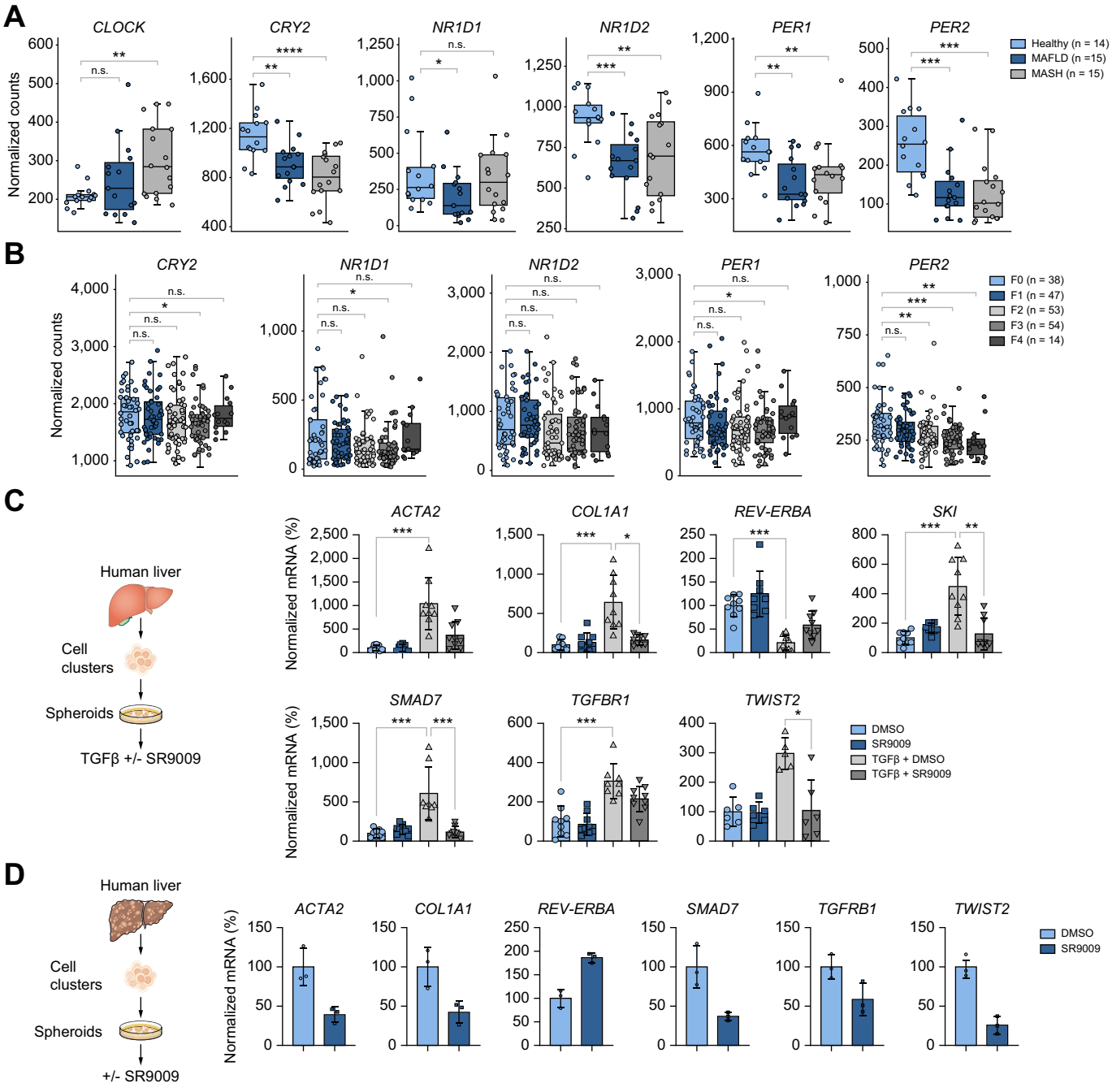

Fig. 8. Expression of CC genes in patients with MASH and pharmacological targeting of the CC in patient liver spheroids. (A) Transcript levels of indicated CC genes in patient livers (GSE126848).[22] Wilcoxon test; *p <0.05, **p <0.01 *** p <0.001 and **** p <0.0001. (B) Transcript levels of indicated CC genes in the livers of patients with varying levels of fibrosis, as indicated (GSE135251).[23] Wilcoxon test; *p <0.05, **p <0.01. (C–D) SR9009 treatment reverses TGF-β-induced CC and profibrotic gene perturbations in patient-derived spheroids. (C) Multicellular liver spheroids were generated from patient liver tissue and treated with TGF-β and SR9009 or DMSO treatment. The graphs show mean ± SD of % of mRNA normalized to *GAPDH* (mock = 100%) from two experiments performed in triplicate (n = 6). *p <0.05, **p <0.01, ***p <0.001 1 Kruskal-Wallis followed by Dunn's multiple comparison tests. (D) Multicellular liver spheroids were generated from cirrhotic liver tissue and treated with SR9009 or DMSO. The graphs show mean ± SD of mRNA normalized to *GAPDH* from one experiment performed in triplicate (n = 3). CC, circadian clock; MASH, metabolic dysfunction-associated steatohepatitis.

Discussion

Our study has the following key findings: (1) the liver CC oscillator 'gates' the expression of TGF-β target genes (Fig. 1 and Fig. S1) in the healthy liver as shown by analyses of *Bmal1KO* and *Rev-Erbα/β*$^{hep-/-}$ CC-mutant mice. Although some of our data are on a correlative level, our functional data from multiple experiments suggest that the CC-controlled pulsatile expression of TGF-β target genes in non-diseased livers may act as a break from driving its constant activity (Figs. 1 and 3), which could otherwise promote fibrosis. (2) MASH metabolic injury perturbs the liver CC which is associated with increased expression of TGF-β target genes (Figs. 2-4). (3) Targeting the liver CC clock provides an opportunity for a previously undiscovered antifibrotic therapy.

Mechanistically, our results suggest that CC oscillators are present in both hepatocytes and HSCs – the key driver cells of liver fibrosis. The alterations of HSC-enriched genes in hepatocyte-specific CC mutants raised the possibility of hepatocyte-HSC crosstalk in which the hepatocyte CC possibly influences HSC gene expression. This hypothesis is further supported by loss-of-function studies in PHH-HLMF co-culture studies although the detailed mechanism remains to be determined (Fig. 5C–E).

We found that TGF-β targets are rhythmically expressed not only in human hepatocytes but also in HSCs. We validated the impact of the human HSC CC oscillator on TGF-β targets by CRISPR-guided KO of CC genes and synchronization experiments (Fig. 4), as a surrogate for *in vivo* HSC-specific CC mutational studies. TGF-β signaling has different biological roles in hepatocytes and HSCs, but includes some common key receptors and effectors, *e.g. Smad7*, *Tgfbr1*. The expression of these common genes indicates 'functional' TGF-β signaling, although whether activation of some of these genes in hepatocytes influences HSC activation during disease remains to be explored. Note that the phase of peak expression for some of these TGF-β target genes are different between mouse and human cells, likely reflecting gene- and species-specific differential enhancer usage. Interestingly, CC regulation of *Tgfb1* and *Smad3* expression has also been observed in the kidney, adipose tissue and heart.[25,26] Genome-wide association studies have implicated different CC genes in various pathologies, including metabolic disease affecting liver and HCC risk.[27] However, an association of CC gene polymorphisms with fibrosis has not been found.

Through multiple approaches we uncovered a "crosstalk" between the CC oscillator and TGF-β signaling. In this crosstalk, the CC component *Rev-Erbs* plays an important role in repressing TGF-β signaling. Moreover, targeting REV-ERBα with a small molecule (SR9009) inhibited liver fibrosis progression in *in vivo* and *ex vivo* models (Figs. 6-8). We chose REV-ERBα as: (*i*) its level was reduced during fibrosis and elevated TGF-β and FFA signaling in mice, patient tissues, HSCs/HLMFs, and PHHs, (*ii*) its activity can be modulated by agonists (SR9009) and (*iv*) such agonists can be safely administered in mice. While the liver CC is known to regulate metabolism, we only observed a modest effect on lipid metabolism upon SR9009 treatment (Figs. 6 and 7) which did not result in a major reduction of liver steatosis *in vivo* (Fig. S14). This is consistent with the well described effect of SR9009 on fatty acid and glucose metabolism predominantly in muscle and adipose tissue.[28] Alternatively, the CDA-HFD model which is designed to study predominantly liver fibrosis[29] may not entirely model the CC's metabolic effects in the liver.

A strength of our study is the validation of results in patient-derived model systems including animal models, spheroids and primary cells, the consistency of results across complementary model systems and patient cohorts supporting its clinical validity and future therapeutic translatability.

The study has the following limitations: (1) While the CDA-HFD is accepted as a state-of-the-art model and widely used to study compounds targeting liver fibrosis, it is limited by only partially modeling MASH metabolism and steatosis,[29] (2) the 2D *in vitro* experiments have limitations including the fact that PHHs de-differentiate during culture and HSCs are rapidly activated. Furthermore, additional studies using combined transcriptome and secretome analyses will be needed to unravel the detailed mechanisms of crosstalk. (3) The study is limited by a lack of HSC-specific KO of CC genes *in vivo*, which could further illuminate the role of HSC 'clock' disruption in liver disease progression. Future studies, *e.g.* in the PDGFRβ CreER mouse model recently developed by Hamberger *et al.*[30] may help to determine whether CC oscillators in hepatocytes and HSCs may be required to de-regulate TGF-β signaling and the regulation of fibrosis-associated genes.

Targeting the CC provides novel opportunities to treat liver fibrosis. A key differentiator of the CC-targeting approach is its antifibrotic efficacy as demonstrated across all models (Figs. 6-8), which addresses a key unmet medical need in the treatment of liver fibrosis. While we did not observe any major adverse effects on liver health, further studies are needed to investigate the safety profile of CC-targeting compounds in patients. Moreover, as our preclinical models are focused on MASH as an etiology for fibrosis, additional studies are needed to show efficacy and impact also in fibrosis of other etiologies, such as chronic viral hepatitis and alcohol-related liver disease. Collectively, our pharmacological proof-of-concept studies across several models, including patient-derived models, uncover the CC as a novel therapeutic target for liver fibrosis – an important unmet medical need.

Affiliations

[1]*University of Strasbourg, Inserm, Institute for Translational Medicine and Liver Disease (ITM), UMR_S1110, Strasbourg, France;* [2]*Department of Medicine II, Gastroenterology, Hepatology, Endocrinology and Infectious Diseases, Freiburg University Medical Center, Faculty of Medicine, University of Freiburg, Freiburg, Germany;* [3]*ÆPIC Animal Facility Platform, University of Strasbourg, Inserm UMR_S1110, Strasbourg, France;* [4]*Department of Gastroenterology, NHO Kure Medical Center and Chugoku Cancer Center, Kure, Japan;* [5]*Hiroshima Prefectural Hospital, Hiroshima, Japan;* [6]*Hiroshima Institute of Life Sciences, Hiroshima, Japan;* [7]*Center for Medical Specialist Graduate Education and Research, Graduate School of Biomedical and Health Sciences, Hiroshima University, Hiroshima, Japan;* [8]*RIKEN Center for Integrative Medical Sciences, Yokohama, Japan;* [9]*Pôle des Pathologies Hépatiques et Digestives, Strasbourg University Hospitals, Strasbourg, France;* [10]*Division of Chronic Inflammation and Cancer, German Cancer Research Center (DKFZ), Heidelberg, Germany;* [11]*Biological Resource Center, Hautepierre, Department of Pathology, Strasbourg University Hospital, Strasbourg, France;* [12]*Groupe Hospitalier Saint Vincent, Strasbourg, France;* [13]*The M3 Research Center, University Tuebingen, Faculty of Medicine, Institute for Interdisciplinary Research on Cancer Metabolism and Chronic Inflammation, M3-Research Center for Malignome, Metabolome and Microbiome, Otfried-Müller-Straße 37, 72076 Tübingen, Germany;* [14]*Cluster of Excellence iFIT (EXC 2180) "Image-Guided and Functionally Instructed Tumor Therapies," Eberhard-Karls University of Tübingen, Tübingen, Germany;* [15]*Institut de Génétique et de Biologie Moléculaire et*

Cellulaire (IGBMC), CNRS UMR7104, Inserm U964, Illkirch, France; [16]*Collège de France, Illkirch, France;* [17]*Institut Hospitalo-Universitaire (IHU) Strasbourg, France;* [18]*Institut Universitaire de France (IUF), Paris, France*

Abbreviations

CDA-HFD, choline-deficient, L-amino acid-defined, high-fat diet; CC, circadian clock; FFAs, free fatty acids; HSCs, hepatic stellate cells; HCC, hepatocellular carcinoma; HLCM, human liver chimeric mouse model; HLMFs, human liver myofibroblasts; LDKO, hepatocyte-specific KO of Rev-Erbα/β; KO, knockout; MASH, metabolic dysfunction-associated steatohepatitis; MASLD, metabolic dysfunction-associated steatotic liver disease; MFs, myofibroblasts; PHHs, primary human hepatocytes; TFs, transcription factors; TGF-β, transforming growth factor-β.

Financial support

The authors acknowledge research support by the European Union (ERC AdG ERC-AdG-2020-FIBCAN #101021417 to T. F. B), the French Cancer Agency (TheraHCC2.0 IHU201901299 to T. F. B), the Agence Nationale de Recherche (ANR-21-RHUS-001 to T.F.B.), the Agence Nationale de Recherche sur le Sida et les hépatites virales (ANRS ECTZ103701, ECTZ131760, ECTZ160436, ECTZ171594 to J.L, ANRS ECTZ104017 to T.F.B.) and USIAS (2020-029, A. M.). K.C was supported by the Japan Agency for Medical Research and Development (AMED) for this work under grant no JP21fk0210090. This work of the Interdisciplinary Thematic Institute IMCBio+, as part of the ITI 2021-2028 program of the University of Strasbourg, CNRS and Inserm, was supported by IdEx Unistra (ANR-10-IDEX-0002), and by SFRI-STRAT'US project (ANR 20-SFRI-0012) and EUR IMCBio (ANR-17-EURE-0023) under the framework of the French Investments for the Future Program as well as state funds managed within the France 2030 program (reference ANR-21-RHUS-0001).

Conflict of interest

The authors declare no conflict of interest.

Please refer to the accompanying ICMJE disclosure forms for further details.

Authors' contributions

T.F.B., A.M., E.C., and J.L. conceived and supervised the study performed at Inserm U1110. P.C. supervised and analyzed experiments done using Bmal1$^{hep-/-}$ mice at IGBMC. T.F.B., A.M., E.C. and M.D. designed experiments. E.C., M.D., C.G., C.P., L.H., M.O. and A.M. performed cell-based and mouse tissue analyses. EC. N.B., R.M., Y.T., H.A., H.A-C. and performed animal experiments, A.S. and F.D.J performed histological analyses. M.O., L.G., T.W. performed histopathologic scoring of mouse livers. S.D. and N.R. processed human liver tissues, S.D., M.O., and D.H. performed histological staining. E.C prepared spheroids from human liver samples for *ex vivo* experiments. M.D., E.C., A.M., T.F.B., C.S. and J.L. analyzed results. F.J. and J.M. performed bioinformatic analyses. P.P. and E.F. provided human liver samples. K.C. provided mouse liver tissues. A.M., E.C., J.L., and T.F.B. wrote the manuscript. All authors edited, read, and approved the submitted manuscript.

Data availability statement

The RNA-sequencing data has been deposited at GEO (GSE264250 for mouse HSC and MF and GSE272293 for MASH/fibrosis model). Data referring to heatmaps and full-length western blots are available in supplementary information. All data are available from the corresponding author upon reasonable request.

Acknowledgements

We acknowledge ÆPIC animal facility platform (University of Strasbourg, Inserm UMR_S1110, Strasbourg, France) for animal experimentation. L'Institut Clinique de la Souris (ICS, Illkirch, France) for mouse plasma analyses, BSF (Vienna, Austria) and Novogene (UK) for RNA-sequencing, and Jenny Hetzer (DKFZ, Heidelberg, Germany) for assistance with IHC. We thank Prof. F. Chisari (The Scripps Research Institute, La Jolla, CA, USA) for providing Huh7.5.1 cells and Céline Roth and Prof. Marie Pierrette Chenard (Centre de Resources Biologiques, CRB, Strasbourg, France) for assistance with histopathology evaluation.

Supplementary data

Supplementary data to this article can be found online at https://doi.org/10.1016/j.jhep.2024.07.034.

References

Author names in bold designate shared co-first authorship

[1] **Hagström H**, **Nasr P**, Ekstedt M, et al. Fibrosis stage but not NASH predicts mortality and time to development of severe liver disease in biopsy-proven NAFLD. J Hepatol 2017;67:1265–1273.
[2] **Roehlen N**, **Crouchet E**, Baumert TF. Liver fibrosis: mechanistic concepts and therapeutic perspectives. Cells 2020;9(4):875.
[3] **Friedman SL**, **Pinzani M**. Hepatic fibrosis 2022: unmet needs and a blueprint for the future. Hepatology 2022;75:473–488.
[4] Sanyal AJ, Van Natta ML, Clark J, et al. Prospective study of outcomes in adults with nonalcoholic fatty liver disease. N Engl J Med 2021;385:1559–1569.
[5] Mukherji A, Bailey SM, Staels B, et al. The circadian clock and liver function in health and disease. J Hepatol 2019;71:200–211.
[6] Weger BD, Gobet C, David FPA, et al. Systematic analysis of differential rhythmic liver gene expression mediated by the circadian clock and feeding rhythms. Proc Natl Acad Sci U S A 2021;118:e2015803118.
[7] **Subramanian A**, **Tamayo P**, Mootha VK, et al. Gene set enrichment analysis: a knowledge-based approach for interpreting genome-wide expression profiles. Proc Natl Acad Sci U S A 2005;102:15545–15550.
[8] Liberzon A, Birger C, Thorvaldsdóttir H, et al. The Molecular Signatures Database (MSigDB) hallmark gene set collection. Cell Syst 2015;1:417–425.
[9] Koike N, Yoo S-H, Huang H-C, et al. Transcriptional architecture and chromatin landscape of the core circadian clock in mammals. Science 2012;338:349–354.
[10] **Mukherji A**, **Kobiita A**, Chambon P. Shifting the feeding of mice to the rest phase creates metabolic alterations, which, on their own, shift the peripheral circadian clocks by 12 hours. Proc Natl Acad Sci U S A 2015;112:E6683–E6690.
[11] Guan D, Xiong Y, Trinh TM, et al. The hepatocyte clock and feeding control chronophysiology of multiple liver cell types. Science 2020;369:1388–1394.
[12] Zhang DY, Goossens N, Guo J, et al. A hepatic stellate cell gene expression signature associated with outcomes in hepatitis C cirrhosis and hepatocellular carcinoma after curative resection. Gut 2016;65:1754–1764.
[13] Aashaq S, Batool A, Mir SA, et al. TGF-β signaling: a recap of SMAD-independent and SMAD-dependent pathways. J Cel Physiol 2022;237:59–85.
[14] **Solt LA**, **Wang Y**, Banerjee S, et al. Regulation of circadian behaviour and metabolism by synthetic REV-ERB agonists. Nature 2012;485:62–68.
[15] **Zhang Y**, **Fang B**, Emmett MJ, et al. GENE REGULATION. Discrete functions of nuclear receptor Rev-erbα couple metabolism to the clock. Science 2015;348:1488–1492.
[16] Dierickx P, Emmett MJ, Jiang C, et al. SR9009 has REV-ERB-independent effects on cell proliferation and metabolism. Proc Natl Acad Sci U S A 2019;116:12147–12152.
[17] Santhekadur PK, Kumar DP, Sanyal AJ. Preclinical models of non-alcoholic fatty liver disease. J Hepatol 2018;68:230–237.
[18] Balaphas A, Meyer J, Gameiro C, et al. Optimized isolation and characterization of C57BL/6 mouse hepatic stellate cells. Cells 2022;11(9):1379.
[19] Zhang YE. Non-smad signaling pathways of the TGF-β family. Cold Spring Harbor Perspect Biol 2017;9(2):a022129.
[20] Newman AM, Steen CB, Liu CL, et al. Determining cell type abundance and expression from bulk tissues with digital cytometry. Nat Biotechnol 2019;37:773–782.
[21] Azuma H, Paulk N, Ranade A, et al. Robust expansion of human hepatocytes in Fah-/-/Rag2-/-/Il2rg-/- mice. Nat Biotechnol 2007;25:903–910.
[22] **Suppli MP**, **Rigbolt KTG**, Veidal SS, et al. Hepatic transcriptome signatures in patients with varying degrees of nonalcoholic fatty liver disease compared with healthy normal-weight individuals. Am J Physiol Gastrointest Liver Physiol 2019;316:G462–G472.
[23] Govaere O, Cockell S, Tiniakos D, et al. Transcriptomic profiling across the nonalcoholic fatty liver disease spectrum reveals gene signatures for steatohepatitis and fibrosis. Sci Transl Med 2020;12:eaba4448.
[24] Roehlen N, Saviano A, El Saghire H, et al. A monoclonal antibody targeting nonjunctional claudin-1 inhibits fibrosis in patient-derived models by modulating cell plasticity. Sci Transl Med 2022;14(676):eabj4221.
[25] **Chen W-D**, **Yeh J-K**, Peng M-T, et al. Circadian CLOCK mediates activation of transforming growth factor-β signaling and renal fibrosis through cyclooxygenase 2. Am J Pathol 2015;185:3152–3163.

[26] Nam D, Guo B, Chatterjee S, et al. The adipocyte clock controls brown adipogenesis through the TGF-β and BMP signaling pathways. J Cel Sci 2015;128(9):1835–1847.
[27] **Janoski JR**, **Aiello I**, Lundberg CW, et al. Circadian clock gene polymorphisms implicated in human pathologies. Trends Genet 2024. S0168-9525(24)00110-0.
[28] Geldof L, Deventer K, Roels K, et al. In vitro metabolic studies of REV-ERB agonists SR9009 and SR9011. Int J Mol Sci 2016;17(10):1676.
[29] **Vacca M**, **Kamzolas I**, Harder LM, et al. An unbiased ranking of murine dietary models based on their proximity to human metabolic dysfunction-associated steatotic liver disease (MASLD). Nat Metab 2024;6:1178–1196.
[30] Hamberger F, Mederacke Y-S, Mederacke I. An inducible model for genetic manipulation and fate-tracing of PDGFRβ-expressing fibrogenic cells in the liver. Sci Rep 2023;13(1):7322.

Keywords: Liver disease; transcriptional regulation; circadian clock; hepatic stellate cells; MASLD; drug discovery.
Received 5 May 2023; received in revised form 18 July 2024; accepted 22 July 2024; available online 22 August 2024